Eli Yakirevich
Turbomachinery and Heat Transfer Laboratory,
Aerospace Engineering Department,
Technion—Israel Institute of Technology,
Technion City,
Haifa 3200003, Israel
e-mail: eliyakir@campus.technion.ac.il

Ron Miezner
Turbomachinery and Heat Transfer Laboratory,
Aerospace Engineering Department,
Technion—Israel Institute of Technology,
Technion City,
Haifa 3200003, Israel
e-mail: ronmi@technion.ac.il

Boris Leizeronok
Turbomachinery and Heat Transfer Laboratory,
Aerospace Engineering Department,
Technion—Israel Institute of Technology,
Technion City,
Haifa 3200003, Israel
e-mail: borisl@technion.ac.il

Beni Cukurel
Turbomachinery and Heat Transfer Laboratory,
Aerospace Engineering Department,
Technion—Israel Institute of Technology,
Technion City,
Haifa 3200003, Israel
e-mail: beni@cukurel.org

Continuous Closed-Loop Transonic Linear Cascade for Aerothermal Performance Studies in Microturbomachinery

The present work summarizes the design process of a new continuous closed-loop hot transonic linear cascade. The facility features fully modular design which is intended to serve as a test bench for axial microturbomachinery components in independently varying Mach and Reynolds numbers ranges of 0–1.3 and 2×10^4–6×10^5, respectively. Moreover, for preserving heat transfer characteristics of the hot gas section, the gas to solid temperature ratio (up to 2) is retained. This operational environment has not been sufficiently addressed in prior art, although it is critical for the future development of ultra-efficient high power or thrust devices. In order to alleviate the dimension specific challenges associated with microturbomachinery, the facility is designed in a highly versatile manner and can easily accommodate different geometric configurations (pitch, ± 20 deg stagger angle, and ± 20 deg incidence angle), absence of any alterations to the test section. Owing to the quick swap design, the vane geometry can be easily replaced without manufacturing or re-assembly of other components. Flow periodicity is achieved by the inlet boundary layer suction and independently adjustable tailboard mechanisms. Enabling test-aided design capability for microgas turbine manufacturers, aerothermal performance of various advanced geometries can be assessed in engine relevant environments. [DOI: 10.1115/1.4037611]

Introduction

For a small gas turbine, in comparison to their larger counterparts, a reduced amount of fluid is supplied to an almost unchanged thermodynamic cycle; hence, the aero-thermo and chemodynamics remain mostly the same. Nevertheless, due to the minimization of the geometric size, a large decrease in Reynolds number is unavoidable. Thus, this not only alters the aerothermal distribution on the blades and vanes but also results in higher viscous losses. Therefore, the components', and hence the cycle's, efficiencies are reduced. In addition to that, above the inherent design complexity associated with all gas turbine engines, the physics associated with mini and microgas turbines are further complicated by dimension-specific challenges, and one of the key technological barriers toward broad-spectrum implementation of microgas turbines is lack of knowledge in aerodynamically coupled heat transfer and thermal management issues.

The present research is concerned with the design of a dedicated facility toward aerothermal assessment of microgas turbine stator performance for both compressors and turbines. Typically, short-duration rigs are a cost-effective way to generate engine similar conditions for a very small temporal frame (typically less than 1 s) and, it is possible to extrapolate the findings to steady aerodynamic operating conditions. Cons of such short duration facilities include difficulties in performing optical measurements due to the reduced test times, characterizing aerothermal performance mapping due to transient conditions, and conducting coupled heat transfer studies—due to large thermal time scales. Addressing these issues, there are a limited number of continuous transonic turbine research rigs, capable of operating in various Reynolds conditions. Regardless of operational principle, a noninclusive list of existing transonic linear cascade facilities in academic institutions is provided in Table 1 [1–12]. The only heated test rigs among them are in Ecole Polytechnique Federal de Lausanne and Virginia Tech [2,11].

According to best knowledge, the existing test section designs mandate a rebuild for every blade profile, as well as stagger angle configuration. This paper describes the design process of a new transonic linear cascade facility at Technion—IIT, specifically targeted for the needs of microgas turbine community. For the typical microgas turbine Reynolds and Mach numbers, $\mathrm{Re} \sim \mathcal{O}(10^4 - 10^5)$ and $M \sim \mathcal{O}(1.05 - 1.35)$, the aerodynamic and thermal performance is highly sensitive to the particular flow conditions, Refs. [13] and [11], respectively. Although the operational principles of some existing facilities (located in Munich and North Dakota [8,9]) can partially address this range, the lower Reynolds and the upper Mach boundaries of the operation envelope have not received much attention. However, these are the critical design aerothermal flow conditions relevant to the microturbomachinery community. In addition, due to restrained research and development costs, cascade test section flexibility to easily accommodate different geometric configurations is a critical mandate, intended to provide scientific advancements in dimension specific challenges of microgas turbines.

Motivation. The efforts to experimentally investigate turbine profile performance have long been a field of interest. Although there exist a multitude of research facilities in academia, as well as the industry, the work presented herein is the first discussion in the open literature devoted to the design, instrumentation, and

Contributed by the Turbomachinery Committee of ASME for publication in the Journal of Engineering for Gas Turbines and Power. Manuscript received July 3, 2017; final manuscript received July 4, 2017; published online September 19, 2017. Editor: David Wisler.

Table 1 Existing transonic linear cascade facilities

Facility location	Exit Re $\times 10^5$	M
Carleton University, Ottawa, ON, Canada [1]	4–10	0.5–1.2
Ecole Polytechnique Federal de Lausanne, Lausanne, Switzerland [2]	10–15	0.7–0.85
German Aerospace Center (DLR), Cologne, Germany [3]	1–30	0.2–1.4
German Aerospace Center (DLR), Gottingen, Germany [4]	7.3–9.4	0.7–1.3
National Aeronautics and Space Administration (NASA), Cleveland, OH [5]	1.7–25	0.2–1.8
Northwestern Polytechnic University, Xian Shi, Shaanxi Sheng, China [6]	4.5–13	0.71–0.91
Royal Military College of Canada, Kingston, ON, Canada [7]	~3.5	0.9–1.12
University of German Armed Forces, Munich, Germany [8]	0.7–11	0.2–1.05
University of North Dakota, Grand Forks, ND [9]	0.5–10	0.5–0.9
University of Oxford, Oxford, UK [10]	8–30	0–1.6
Virginia Tech, Blacksburg, VA [11]	6–11	0.55–1.05
Von Karman Institute (VKI), Rhode-Saint-Genèse, Belgium [12]	5–34	0.3–1.25

operational characteristics of a hot closed-loop continuous transonic turbine cascade geared specifically toward advanced aerothermal performance studies in microturbomachinery.

The unique versatile test facility features presented in the scope of this work significantly reduce the turnaround time between different experimental campaigns and provide the research community with a reliable tool that simulates the aerothermal parameters relevant to microturbomachinery. In the future, this will yield a large empirical database, which can be used for computational fluid dynamics validation.

The present paper offers an extensive description of design choices and guidelines necessary toward future developmental efforts. The ultimate goal of the article is to communicate the knowledge gained throughout the facility design process (as well as the arising guidelines) to the research community and facilitate future efforts in the field of experimental microturbomachinery.

Facility Requirements. The goal of the planned facility is to create a platform for versatile test aided design of compressor stators, and more importantly turbine nozzle guide vanes. Along these lines, the capabilities are geared toward convenient aerodynamic performance studies including improved transonic loss correlations, as well as evaluation of heat transfer characteristics under a broad range of thermal management (cooling) techniques.

The Technion transonic linear cascade (TTLC) differs from the already existing facilities in several unique ways. In order to capture the changing loading conditions, as well as the potentially varying vane geometry, the facility is designed to provide effortless modification of incidence and stagger angles (in the range of ± 20 deg), absence of any alterations to the test section. Furthermore, the considered vane geometry can be easily replaced owing to the quick swap design, which permits the cascade to be rebladed without manufacturing or re-assembly of other components. At the exhaust, the cascade outlet has to accommodate a large range of flow turning angles, in order to address the needs of both compressor and turbine stators.

In addition to the versatility requirements, to enable more straightforward aerothermal measurements, the test rig is expected to operate continuously, providing periodic conditions (lack of transverse spatial velocity and pressure gradients) over at least two passages surrounding an airfoil. Due to mass flow limitations, TTLC has to implement a finite number of blades. Based on design guidelines [14], typical axial turbomachinery profiles can be effectively imitated by a set of individual blades.

Since it is highly impossible to design a fixed-framed cascade for different sized vanes, similarity principles are used to scale the dimensions of the components [15] through preservation of Re and M numbers. By independent control of these two nondimensional quantities, different aerodynamic conditions can be simulated. Moreover, for preserving heat transfer characteristics of the hot gas section, in addition to the purely aerodynamic variables, it suffices to retain the gas to solid temperature ratio. Therefore, TTLC is required to maintain true M–Re–T_{ratio} independency. Finally, in the research and development framework, easy introduction of intrusive and nonintrusive measurement techniques is mandatory.

Turbine Research Facility

Facility Layout. In order to vary Re and M numbers independently, the dimensional quantities which need to be influenced are flow velocity and density. In continuous open-loop systems, as exhaust pressure is atmospheric, these system conditions are directly coupled. In abundance of available pressurized air, the backpressure can be adjusted via an ejector, which has a typical entrainment efficiency of ~30%. However, when the mass flow rate is highly limited, the only feasible solution to attain Re–M independence is operation in a closed-loop configuration, where the control parameters are compressor speed and total mass present in the cycle.

In order to move the fluid through the system volume at a range of nominal pressures, a rotary type positive displacement machine is desirable due to its nearly vertical operating line. Therefore, it can provide relatively constant volumetric flow for a range of inlet pressures at a given rotational speed. In literature, a Roots type blower has been prior considered for cascade studies [9]. However, although it is capable of providing sufficient mass flow, the attainable pressure ratio does not typically exceed 2:1. Considering that most microturbine vanes operate at M number range of 1.1–1.3, the delivered pressure rise is insufficient. Consulting the specific diameter–specific speed charts [16], the selected drive configuration is a variable speed screw type compressor that provides mass flow rate of 0.9 kg/s at up to 7:1 pressure ratio within an inlet pressure range of 0.3–1 bar. Moreover, anticipating the requirements of the future rotating turbine test facility in Technion, the delivered pressure ratio is expected to suffice the forecasted needs.

The schematic layout of the closed test facility and its components are presented in Fig. 1, comprising of the two-stage oil

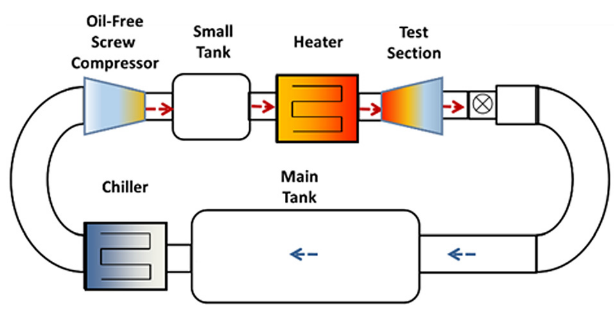

Fig. 1 Closed-loop TTLC facility layout

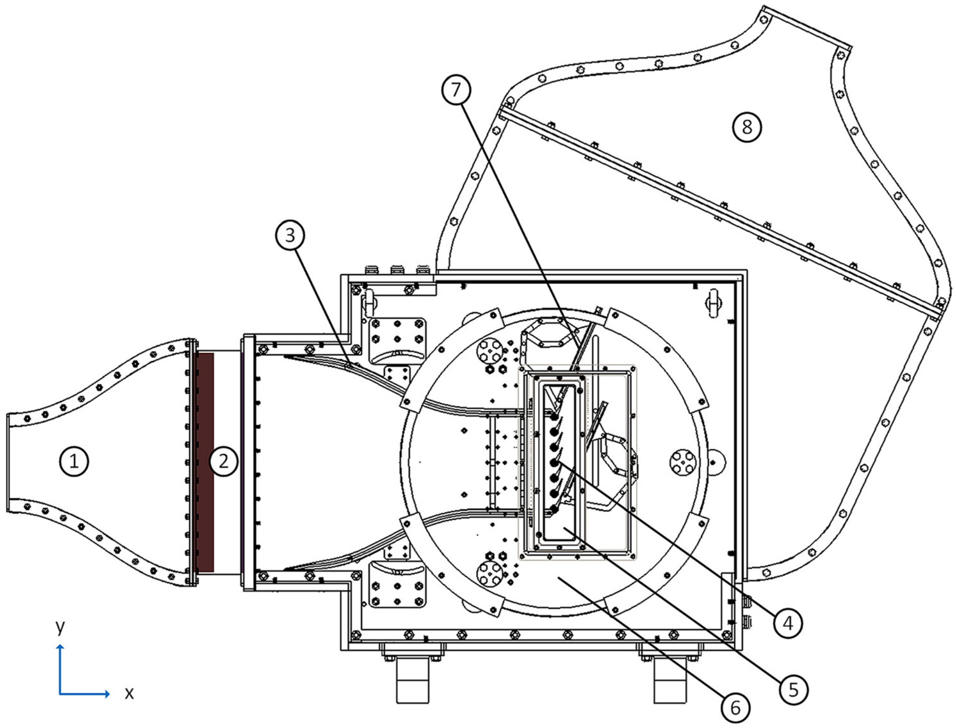

Fig. 2 Technion transonic linear cascade test section layout and reference frame

free screw compressor, small 6 m^3 pressure equalization tank to damp out transients, electric 350 kW heater, test section, pressure drop valves, large 24 m^3 dump tank, and aftercooler, which reduces the compressor inlet temperature to 300 K. Considering the aerodynamic similarity parameters, the volumetric flow rate (and therefore M) is predominantly set by the compressor rotational speed, whereas the total mass in the isolated system defines the Reynolds number. The air retained in the cycle is coarsely adjusted during start-up by a blow-off valve, and fine-tuned during operation. The pressure ratio is determined by the cascade and piping losses, as well as the pressure drop valve setting which prevents compressor inlet from over-pressurizing. For matching nondimensional thermal conditions in the test section, the process heater can bring the flow temperature up to 650 K. In summary, the system control parameters are compressor speed, total enclosed mass together with the pressure drop valve, and the electric heater power, which prescribe the desired M, Re, and T_{ratio}, respectively.

Mechanical Design

The cascade features a modular design, able to accommodate a wide range of compressor stator and turbine vane configurations. The main test section subassemblies and the reference frame used are presented in Fig. 2. The subsections include an inlet (1), flow straightener and turbulence grid (2), controllable main frame frontboards (3), bladed test section (4), optical access window (5), rotating disks (6), controllable main frame tailboards (7), and an outlet (8). The modules are designed to interface with other components with sufficient tolerance $\mathcal{O}(10^{-5}\,\mathrm{m})$ to not hinder operability, while preventing undesired movement between subsections. Stainless Steel 304 with a nominal thickness of 17 mm is selected as the primary manufacturing material due to its mechanical properties, affordability, machinability, and stain resistance.

Inlet. Inlet flow characteristics are crucial factor for the test section performance. The flow enters the contraption through a standard 6 in diameter flange, and the cross-sectional area is reduced by 28% in a linear fashion to provide flow in a high aspect ratio rectangular slot of 30 mm × 440 mm. The inlet is designed to produce attached uniform flow with minimal boundary layer thickness. This is achieved by the bellmouth shape with zero gradient solid boundary conditions [17,18], where the air is expanded in the *XY* plane, while contracting in the *XZ* plane. In this configuration, the Bell–Mehta guidelines describe the contraction plane profile, while the expansion shape is dictated by the linear area change. The design was tested using FloEFD RANS solver developed by Mentor Graphics. It utilizes a modified k–ε two-equation turbulence model (where turbulence intensity (I) is 2% and turbulence length scale (l) is 2 mm) in association with immersed boundary Cartesian meshing technique, coupled with a two-scale wall function treatment. The average dimensionless wall distance (y^+) was 125. Since the entry length of the input pipe is less than five diameters, the incoming flow was assumed to

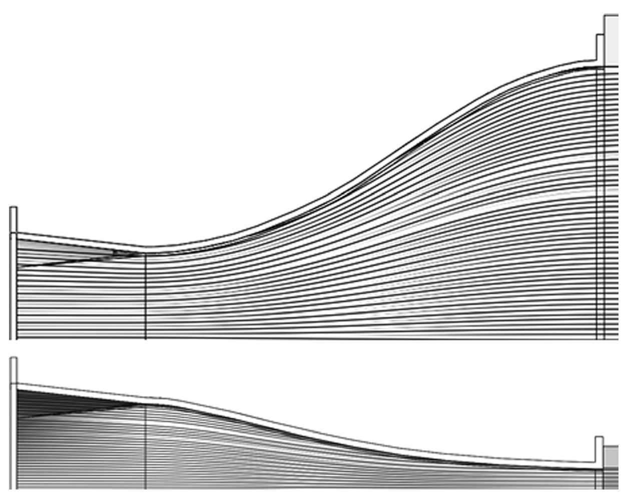

Fig. 3 Flow lines across the inlet *XY* (top) and *XZ* (bottom) cross sections

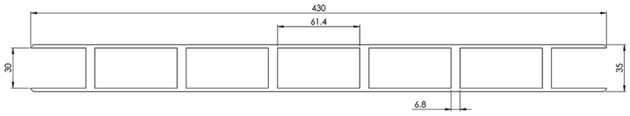

Fig. 4 Turbulence grid design (mm)

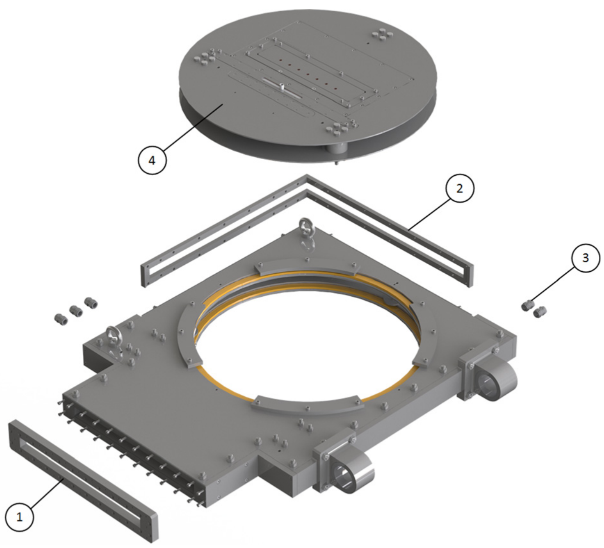

Fig. 5 Main frame assembly

be uniform [19]. The simulations results are presented in Fig. 3, and no observable separation is present in the flow path.

Due to high cross-sectional perimeter to area ratio, the pressure loads on the inlet need to be addressed. Finite elements analysis was conducted using the internal static solver of SOLIDWORKS CAD design software for the highest operational pressure conditions. The resulting deflections less than 0.25 mm can be considered aerodynamically negligible, whereas the ensuing stresses (of 60 MPa order) yield infinite life according to S–N diagram with a von Mises criterion based safety factor of 5.

Honeycomb is a typical component for most wind tunnel designs due to its ability to negate cross-flow vortices [20], which are typically created due to upstream geometrical changes. Due to lateral turbulence inhabitance and pressure loss considerations, the implemented honeycomb design consists of 3.2 mm hexagonal aluminum cells with size to length ratio of 10, as proposed by Refs. [21–26].

Finally, in a typical turbomachine, different components have varying turbulence intensity levels. The first compressor stage usually has very little turbulence, whereas the last turbine stage experiences much higher levels due to the upstream combustor and stages. Therefore, in order to mimic the turbulence intensity of various engine relevant conditions, the cascade includes a modular turbulence grid, situated downstream of the honeycomb. Based on the criteria set in Ref. [27], a representative turbulence grid is depicted in Fig. 4, simulating typical first turbine rotor vane's turbulence intensity of 5% [28].

Main Frame and Rotating Disks. The main frame is the load bearing component, as it provides mechanical interface and support for the other subassemblies and measurement devices (Fig. 5). It includes inlet (1) and outlet (2) sealed mechanical interfaces, electric and pressure cabling ports (3), and rotating disks (4) that confine the cascade. The disks are installed on self-lubricating bronze bearings and allow rotational movement of the test section to accommodate changes in incidence angles. The rotating disks' modular window provides optical access in both the visual and infrared ranges.

Disk Rotation Mechanism. The disk rotation mechanism is designed to allow positioning within the required ± 20 deg incidence angle range. The concept is based on a metallic thread connected to a stepper motor fixed on the main frame. The freely rotating housing of the actuator allows translating a linear motion of a nut to circular movement of the disk assembly (Fig. 6). To overcome potential friction forces, the linear motor is able to generate force of 1200 N.

Frontboard Design. As a result of the disk rotation, the frontboards are to be maintained sealed and parallel for all incidence angles (Fig. 7). Three modules keep the walls leak-proof and aligned for all conditions. Movable Teflon seals (A) keep the walls leak-proof, while the positioning mechanism (B) and leaf springs (C) translate the circular motion of the disks to parallel movement of the boards.

Two distinct configurations were considered during the frontboard design process—bellmouth curved and straight shaped.

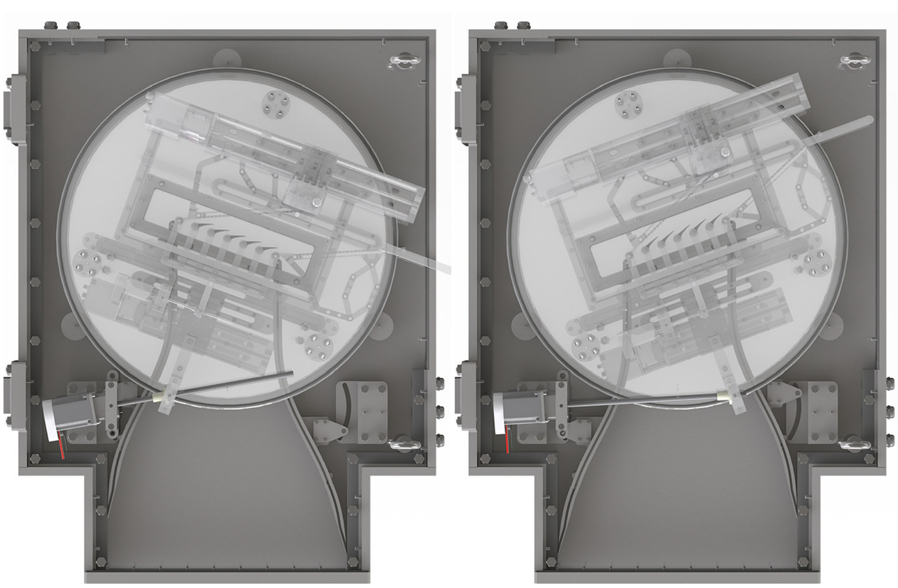

Fig. 6 Disks rotation mechanism set to ± 20 deg

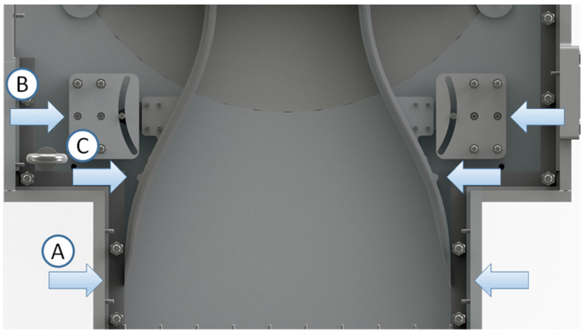

Fig. 7 Frontboards sealing and support mechanisms

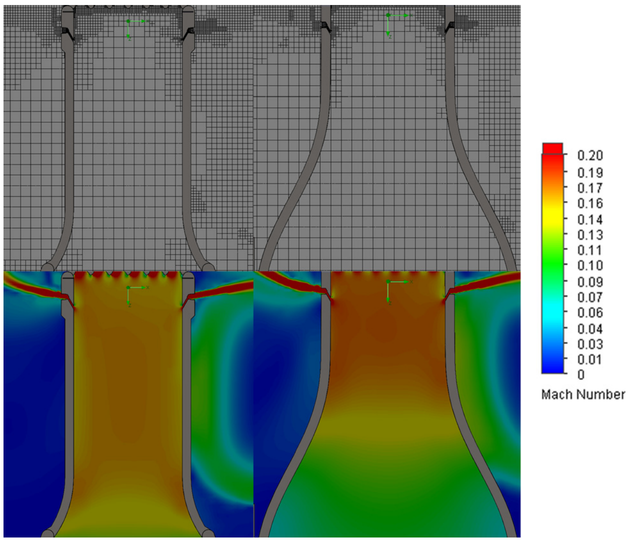

Fig. 8 Frontboard *XY* flow simulation: mesh and results for straight frontboards (left) and bellmouth shaped frontboards (right)

The simulation results are presented in Fig. 8 for both shapes. Based on the reduced boundary layer development, the bellmouth configuration was selected as the frontboard design choice.

Nevertheless, the frontboards boundary layers may cause partial blockage of the far side test section passages, such that they no longer contribute to periodicity [14]. An additional simulation was conducted to quantify the boundary layer thickness in the *XY* and *XZ* planes (Fig. 9). At three chords upstream of the test section, the boundary layers in the *XY* plane cover 12% of the pitch in the two far most passages. In order to overcome this issue, a slanted boundary layer suction mechanism is implemented at the end of the frontboards before the test section at two chords upstream of the test section. The air is ingested (up to 4% of overall flow rate) through a thin slot, the mass flow of which is regulated by an external valve. This mechanism can effectively purge the entire momentum deficit. However, it is challenging to suck the boundary layer in the *XZ* direction, while preserving the total air mass in the closed system. Nevertheless, at the immediate upstream of the test section, the top and bottom boundary layers cover 30% of the span in total, resulting in two-dimensional (2D) flow in the remainder 70% of the blade height. Hence, the cascade is suitable toward aerothermal investigation of various 2D airfoil profiles.

Observation Window. The considered airfoil geometry is mounted on a window, which is bolted onto the rotating disks through a frame interface (Fig. 10). For optical measurements in

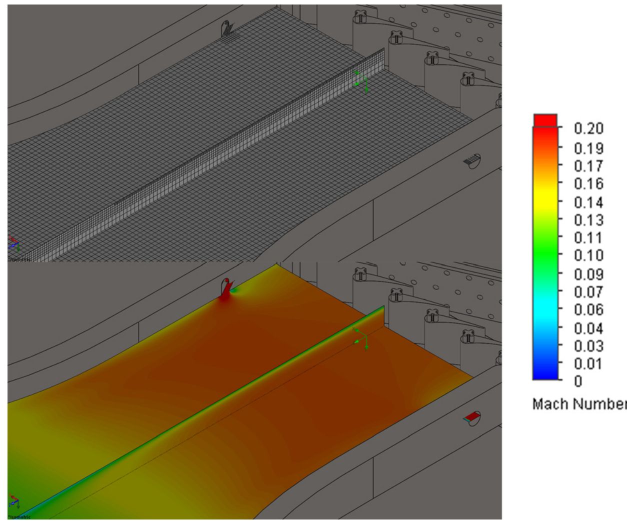

Fig. 9 Frontboard three-dimensional flow simulation: mesh and results for bellmouth shaped frontboards

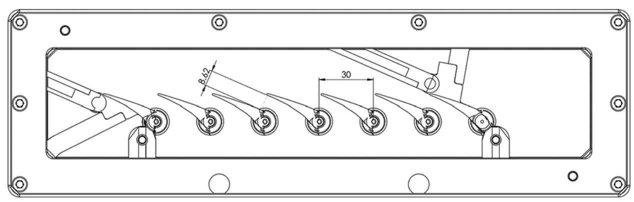

Fig. 10 Test section window frame

the infrared and visible spectra, a transparent ceramic made of alumina oxide is used. The wavelength range which exceeds 75% transparency is from 0.35 to 4.0 μm. The opening can be substituted by a metal blank when no optical access is required.

Since the hub and tip surfaces of the vanes are not constrained, the tip clearance presents major structural requirement, in addition to the general stress considerations. The 17 mm thick stainless steel plates provide sufficient structural strength, with a von Mises safety factor of 15, as predicted by the finite elements analysis simulation. As the yield strength of alumina oxide is orders of magnitude larger than steel, the window has no significant impact on the analysis. Based on the computed displacements at maximal operational pressure, the estimated tip clearance is 0.08 mm—less than 0.3% of the vane height.

Vanes Assembly. To conduct preliminary validation of the test facility's design and operation, the transonic and highly loaded NASA C3X vane geometry is considered, for which aerothermal performance data are publicly available [29]. According to the guidelines described in Ref. [14], six blade passages are sufficient

Table 2 Vane geometry comparison

Parameter	C3X vane	TTLC vane
Axial chord, Cx (mm)	78.16	19.9
True chord (mm)	144.93	36.9
Pitch, *S* (mm)	117.73	30
Span, *H* (mm)	76.2	30
Solidity, Cx/*S*	0.66	0.66
Aspect ratio, *H*/Cx	0.975	1.5
Throat dimension (mm)	32.92	8.61
Setting angle (deg)	59.89	59.89
Air exit angle (deg)	72.38	72.38

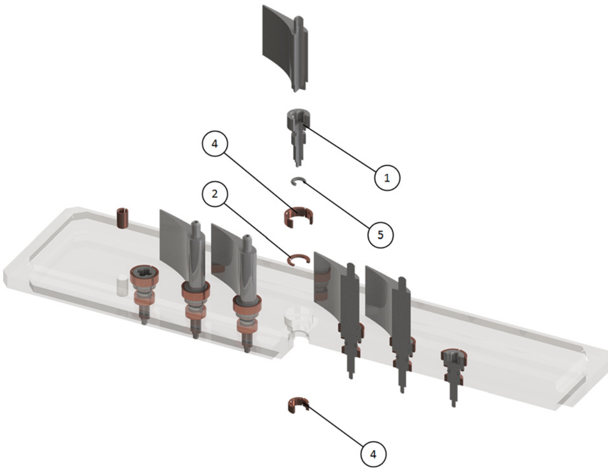

Fig. 11 Vane mounting and friction bearings setup

to attain flow periodicity around the center vane. The 2D profiles are scaled down, such that the solidity (axial chord to spacing ratio) is maintained while the blade aspect ratio is varied due to mass flow choking considerations. The resulting scaled geometry is summarized in Table 2. The larger aspect ratio is a common feature of linear cascade testing, intentionally elongated blades attempt to minimize hub and tip boundary layer effects.

According to the profile loading distribution, the blades are subjected to an 8 kg force, yielding negligible torque and stress values. Figure 11 shows the vanes installed on the window

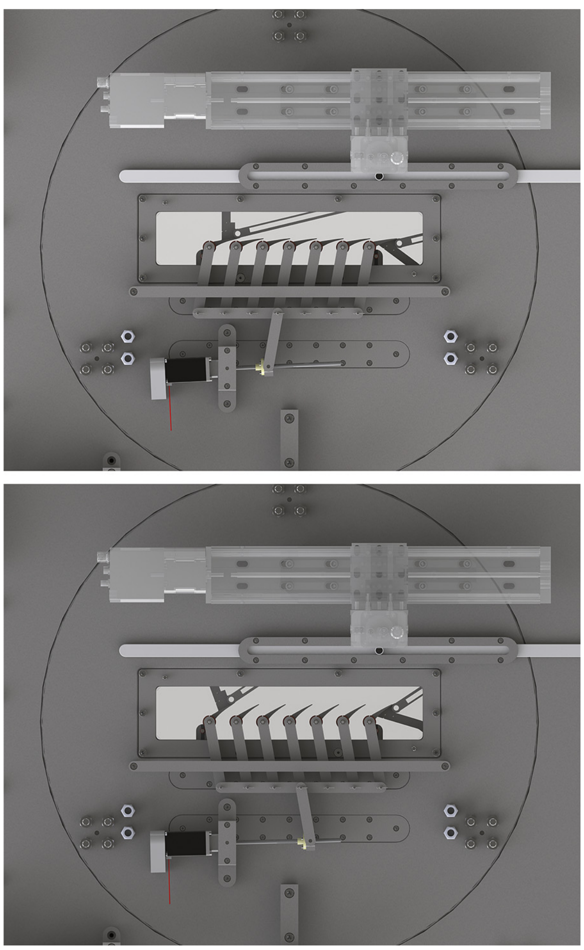

Fig. 12 Stagger control mechanism set to ±20 deg

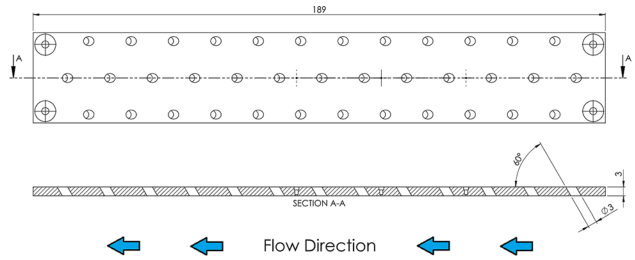

Fig. 13 Tailboards design features

using a set of vane mounts (1), self-lubricating bronze bearings (2, 3, 4), and an O-ring (5). Tolerances of the blade-mount interface are critical, as every 5 μm translates to 0.1 deg rotation of the vane trailing edge, resulting in a 1% change in throat area.

Stagger Control. To accommodate the requirement for stagger angle variations, which are particularly relevant for future variable nozzle guide vanes investigations, each airfoil mount is connected through a mechanism, which resembles typical inlet guide vane actuators found in gas turbines (Fig. 12). The stepper motor generates 300 N and allows stagger angle variation in the range of ±20 deg.

The error induced by the stagger control mechanism is an order of magnitude smaller than the inaccuracy due to improper blade mounting ($\mathcal{O}(0.01^0)$ for 0.1 mm). Hence, the tolerance of the stagger angle regulator is less critical.

Tailboards. The purpose of the tailboards is to confine the jet at the exhaust of the test section. It is a crucial procedure for temporal stability and spatial periodicity [14]. However, the introduction of tailboards causes shockwave reflections from the solid boundaries and promotes undesirable pressure fluctuations [30]. In order to negate this effect, which is an artifact of the test conditions, the tailboards include 3 mm perforations at 60 deg incline to the flow (Fig. 13). With 6% free area ratio, and tailboard thickness to hole diameter of 1, the pressure gain in the shock wave is effectively dissipated inside the hole cavities [31]. However, in order for this process to result in full pressure wave cancelation, the tailboards must be set at an angle representing the flow streamlines. In transonic regime, the flow deflection angle is a function of local M number, which is unknown a priori. Therefore, the tailboard angle can be fine-tuned during the experiment using a scissor leverage mechanism (Fig. 14). The physical restrictions of the main frame resulted in a design that allows a relatively small

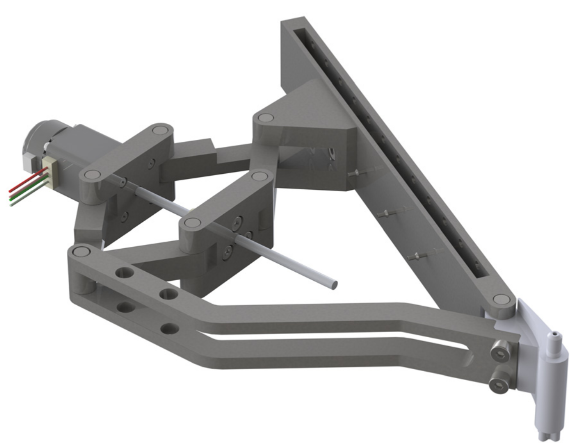

Fig. 14 Tailboards angle control mechanism

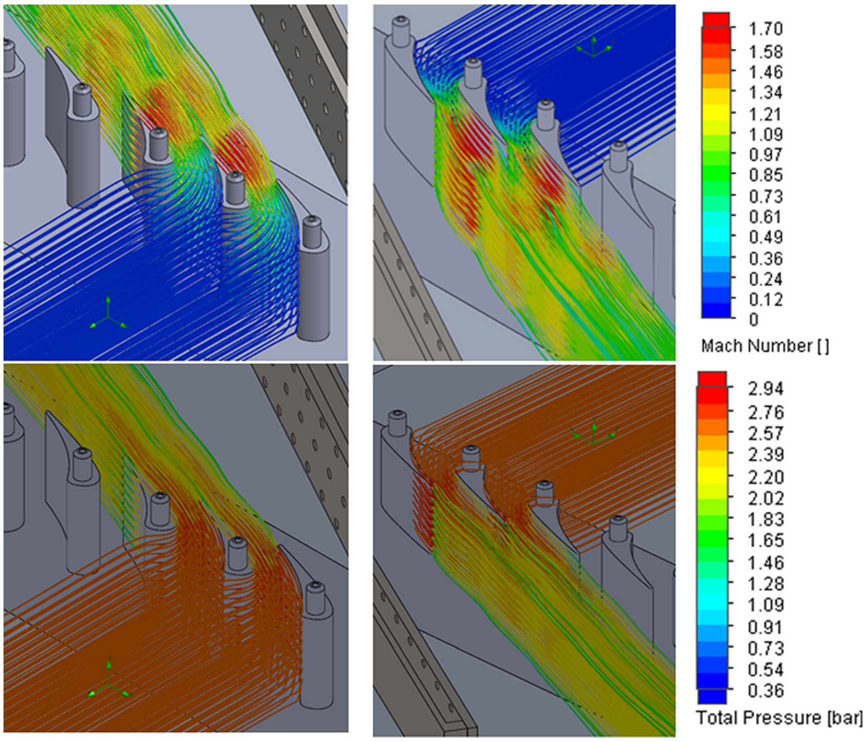

Fig. 15 Mach (top) and total pressure (bottom) distribution in the streamlines

linear actuator, capable of generating only 100 N, to withstand the forces created by the transonic flow.

Flow Periodicity. The flow behavior and the validity of the experimental data are heavily influenced by the spanwise flow characteristics upstream and downstream of the test section [14,32]. The inlet boundary layer suction maintains relatively uniform 2D pressure and velocity distributions across all six passages. Together with exit tailboard actuation, the final design can achieve downstream periodicity in all stagger and incidence angle configurations. According to RANS simulations under nominal design conditions, Fig. 15 depicts stream-tubes colored by local Mach and total pressure distributions over the two middle passages. Periodicity is expected to be achieved within 5% in M distributions.

Outlet Design. The outlet is a transition piece which ducts the flow from the high aspect ratio rectangular test section to a standard 6 in pipe (Fig. 2). The equilateral design of the outlet—main frame interface allows two outlet configurations (Fig. 16), which are suitable for both turbine and compressor studies and their respective flow turning angles.

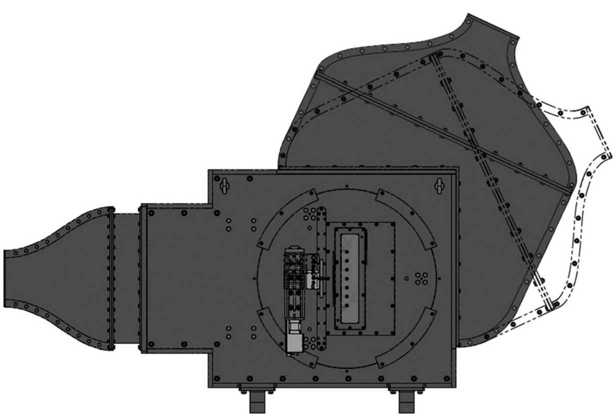

Fig. 16 Outlet configuration for compressor and turbine stators

Sealing. The sealing materials were selected to conform to the general TTLC requirements. The inlet, main frame, and the outlet are sealed using custom rubber gaskets. To allow movement and prevent unwanted leaks, the nonstationary frontboards are sealed using Teflon and the rotating disks feature double O-ring design that prevents leakages from both sides of the bronze bearing.

Measurements Design

This section presents the measurement techniques accommodated in TTLC facility, with particular attention to minimal flow disturbance due to small dimensional scales. Aerodynamic performance measurements are to precisely acquire local and global flow parameters (i.e., velocity, density, pressure), whereas thermal performance can be gauged by assessing temperature changes in the fluid and on the solid surface, as well as cooling effectiveness by observing the associated mixing.

Operational Health Monitoring. Operational health monitoring measurements are designed to ensure stable, continuous, and periodic flow at the inlet and exit of the test section. In this light, mass flow rate, total pressure, and temperature are measured at the upstream 6 in air supply pipe. In addition, three sets of differential pressure measurements from the two porous tailboards are used as a guideline to achieve flow periodicity, which is confirmed by an array of 30 static pressure taps upstream and downstream of the vanes (Fig. 17). To provide correct static pressure measurements with minimal flow interference, the static pressure ports follow the guidelines suggested in Ref. [33]. Due to small port dimensions and structural considerations, the hole length (l) and the hole diameter (d) is set to 0.5 mm, limiting the pressure measurement error to ∼0.3%.

Aerodynamic Performance. In order to quantify integral loss, the total pressure distribution is measured by a sealed YZ traverse

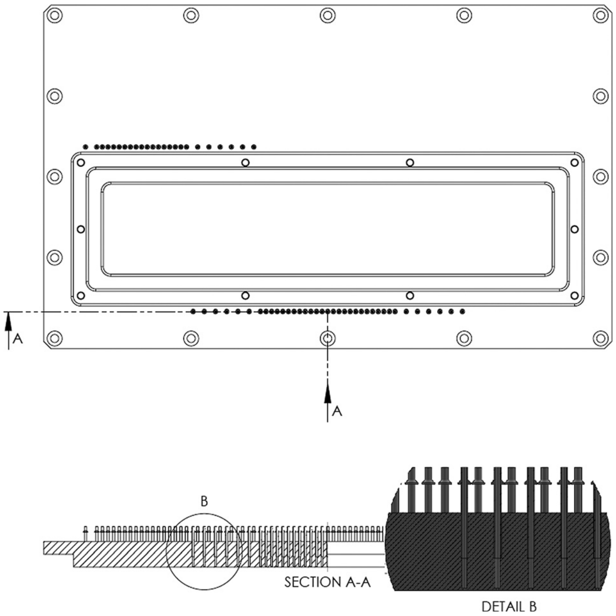

Fig. 17 Static probes arrangement

that is equipped with a miniature five-hole probe, orange arrow in Fig. 18. The measurement ports are located at 2 and 4 chord distances at upstream and downstream of the airfoils, spanning the entire pitchwise direction. Considering the 1.6 mm probe diameter, the blockage effect can be evaluated in terms of pressure measurement error [14]. At inlet $M \sim 0.2$, the upstream total pressure error is estimated to be in the order of $\pm 2\%$ for the 5% blockage ratio. In the transonic wake of the vanes, the measurement probe has to be calibrated in flow specific conditions. Therefore, due to the dimensional restrictions, nonintrusive measurements are desirable. Along these lines, the test section windows are designed to

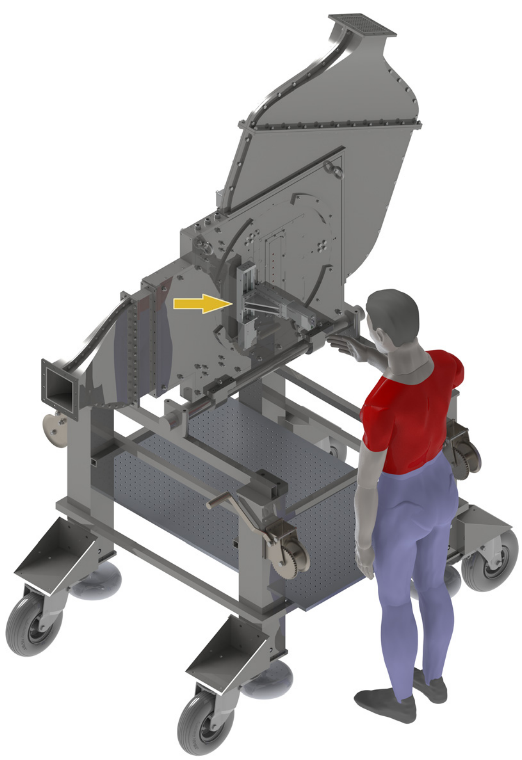

Fig. 18 Cascade assembly in basic operation

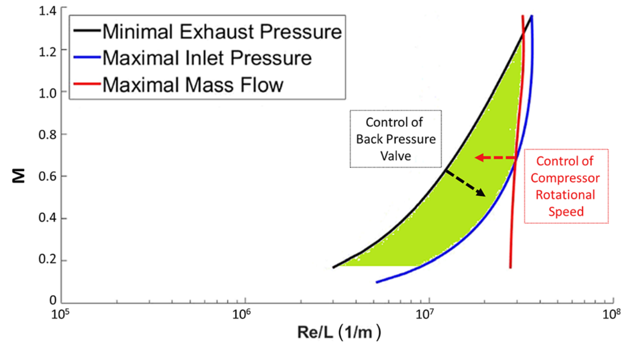

Fig. 19 Technion transonic linear cascade open-loop operational envelope

enable optical access for quantitative Schlieren imaging and particle image velocimetry.

Thermal Performance. Several measurement methods are considered to evaluate the thermal performance of the test geometry. Infrared thermography can provide surface temperature distributions. Furthermore, cooling effectiveness of advanced internal and external thermal management techniques can be assessed by surfaces embedded microhot film sensors. Finally, the film cooling effectiveness is to be studied by the pressure sensitive paint technique [34,35], which is sensitive to partial pressure of oxygen and characterizes the coolant mixing into the freestream through introduction of CO_2 into vane cooling passages.

Cascade Operation Envelope

There are three main factors that present limitations on the facility operation: the maximal available flow rate, the highest attainable inlet pressure, and the minimal possible exhaust pressure. The limitations can be used to present the TTLC operational envelope in $M - Re/L$ space [36]. For the open-loop configuration, the operational envelope is presented in Fig. 19, where the outlet pressure is limited by the atmospheric conditions.

Several controls are used to set the operating point within the available range. Screw compressor's rotational speed can be adjusted to directly control the mass flow supply into the system. Downstream back pressure valve is used to control the static to total pressure ratio. The resultant operation point is located at the intersection of the mass flow and the exhaust pressure lines.

In order to accommodate a larger range of Reynolds variations, as typically observed in microgas turbine applications, the system is designed to operate in closed-loop configuration. Reduction of the total fluid amount in the system, by venting the extra mass through the compressor discharge valve, will decrease the density of the flow. This is enabled by the custom-built compressor, which can operate with inlet pressure in the range of 0.3–1.2 bar. Due to

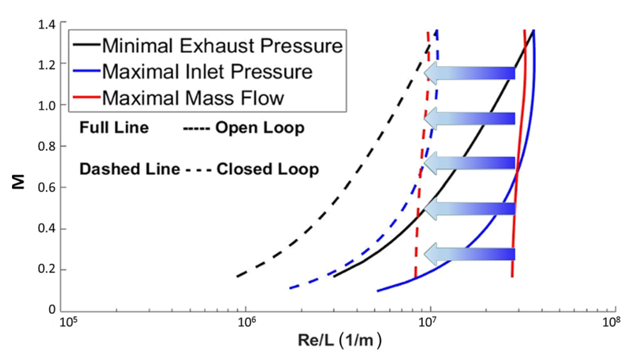

Fig. 20 Closed-loop operational envelope manipulation

the volumetric nature of the pressure rise process, the total mass flow rate drops linearly. However, the choked flow relations also capture this effect, and the resultant M number is unaffected, whereas the Re number decreases, Fig. 20. The final operational range is $0 < \mathrm{M} < 1.3$, $10^6 < \mathrm{Re}/L < 3 \times 10^7$; and considering typical axial chord of 20 mm, the ensuing Re range is 2×10^4 -6×10^5. These values cover the typical operational range of microturbomachines.

Summary

The present work deals with the aerothermal assessment of microgas turbine stator performance, for both compressors and turbines. This effort is structured around the design of a versatile closed-loop pressurized transonic test facility, which provides unique research capabilities to the global research environment. To this end, an adaptive wind tunnel test section is capable of accommodating independently variable stagger and incidence angle conditions, and interchangeable airfoil profiles, to enable test-aided design capability for engine manufacturers.

The facility operates through the drive of a variable-speed compressor, which creates pressure ratios of up to 7:1, with a maximum flow rate of 0.9 kg/s. The closed-loop nature of the facility allows independent Mach and Reynolds variations within an operation range ($0 < \mathrm{M} < 1.3$, $2 \times 10^4 < \mathrm{Re} < 6 \times 10^5$) particularly relevant to microgas turbines. Moreover, to enable heat transfer studies, the test section flow temperature can be raised up to 650 K, yielding gas to solid temperature ratio of 2.

In the near future, TTLC will be validated using the well-documented NASA C3X vane profile. After the verification of the preliminary experimental findings, the facility will be instrumented by a large selection of measurement techniques to document the aerothermal performance of various advanced microturbine geometries in engine relevant environments.

Funding Data

- Minerva Foundation (Grant No. AZ5746940764).

References

[1] Jouini, D., Sjolander, S., and Moustapha, S., 2000, "Aerodynamic Performance of a Transonic Turbine Cascade at Off-Design Conditions," ASME Paper No. 2000-GT-0482.
[2] Vogel, G., 2002, "Experimental Study on a Heavy Film Cooled Nozzle Guide Vane With Contoured Platforms," Ph.D. thesis, Ecole Polytechnique Federale de Lausanne (EPFL), Lausanne, Switzerland.
[3] Schreiber, H.-A., Steinert, W., and Küsters, B., 2000, "Effects of Reynolds Number and Free-Stream Turbulence on Boundary Layer Transition in a Compressor Cascade," ASME Paper No. 2000-GT-0263.
[4] Detemple-Laake, E., 1991, "Detailed Measurements of the Flow Field in a Transonic Turbine Cascade," ASME Paper No. 91-GT-029.
[5] Giel, P. W., Boyle, R. J., and Bunker, R. S., 2003, "Measurements and Predictions of Heat Transfer on Rotor Blades in a Transonic Turbine Cascade," ASME Paper No. GT2003-38839.
[6] Liu, C., Zhu, H. R., Fu, Z. Y., and Xu, R. H., 2015, "The Effects of Inlet Reynolds Number, Exit Mach Number and Incidence Angle on Leading Edge Film Cooling Effectiveness of a Turbine Blade in a Linear Transonic Cascade," ASME Paper No. GT2015-42888.
[7] Woodason, R., Asghar, A., and Allan, W., 2009, "Assessment of the Flow Quality of a Transonic Turbine Cascade," ASME Paper No. GT2009-60164.
[8] Mack, M., Niehuis, R., Fiala, A., and Guendogdu, Y., 2013, "Boundary Layer Control on a Low Pressure Turbine Blade by Means of Pulsed Blowing," ASME J. Turbomach., **135**(5), p. 051023.
[9] Mihelish, M., and Ames, F., 2013, "The Development of a Closed Loop High Speed Cascade Wind Tunnel for Aerodynamic and Heat Transfer Testing at Moderate to Low Reynolds Numbers," ASME Paper No. GT2013-95048.
[10] Povey, T., Oldfield, M., and Haselbach, F., 2008, "Transonic Turbine Vane Tests in a New Miniature Cascade Facility," Proc. Inst. Mech. Eng., Part A, **222**(5), pp. 529–539.
[11] Carullo, J., Nasir, S., Cress, R. D., Ng, W. F., Thole, K. A., Zhang, L. J., and Moon, H. K., 2011, "The Effects of Freestream Turbulence, Turbulence Length Scale, and Exit Reynolds Number on Turbine Blade Heat Transfer in a Transonic Cascade," ASME J. Turbomach., **133**(1), p. 011030.
[12] Paniagua, G., Sieverding, C., and Arts, T., 2013, "Review of the Von Karman Institute Compression Tube Facility for Turbine Research," ASME Paper No. GT2013-95984.
[13] Dixon, S. L., and Hall, C., 2013, *Fluid Mechanics and Thermodynamics of Turbomachinery*, Butterworth-Heinemann, Oxford, UK.
[14] Hirsch, C., 1993, "Advanced Methods for Cascade Testing," Specialised Printing Services Limited, Loughton, UK, No. AGARD-AG-328.
[15] White, F. M., and Corfield, I., 2006, *Viscous Fluid Flow*, Vol. 3, McGraw-Hill, New York.
[16] Kenneth, E., and Nichols, P., 2012, "How to Select Turbomachinery for Your Application," Barber-Nichols Inc., Arvada, CO, pp. 5–6.
[17] Brassard, D., and Ferchichi, M., 2005, "Transformation of a Polynomial for a Contraction Wall Profile," ASME J. Fluids Eng., **127**(1), pp. 183–185.
[18] Bell, J. H., and Mehta, R. D., 1988, "Contraction Design for Small Low-Speed Wind Tunnels," Stanford University, Stanford, CA, Technical Report No. NASA-CR-182747.
[19] Al-Nassri, S., and Unny, T., 1981, "Developing Laminar Flow in the Inlet Length of a Smooth Pipe," Appl. Sci. Res., **36**(5–6), pp. 313–332.
[20] So, R. M., and Mellor, G. L., 1973, "Experiment on Convex Curvature Effects in Turbulent Boundary Layers," J. Fluid Mech., **60**(1), pp. 43–62.
[21] Rae, W. H., and Pope, A., 1984, *Low-Speed Wind Tunnel Testing*, Wiley, Hoboken, NJ.
[22] Mehta, R. D., and Bradshaw, P., 1979, "Design Rules for Small Low Speed Wind Tunnels," Aeronaut. J., **83**(827), pp. 443–453.
[23] Fournier, R. L., 2011, *Basic Transport Phenomena in Biomedical Engineering*, CRC Press, Boca Raton, FL.
[24] Loehrke, R., and Nagib, H., 1976, "Control of Free-Stream Turbulence by Means of Honeycombs: A Balance Between Suppression and Generation," ASME J. Fluids Eng., **98**(3), pp. 342–351.
[25] Bernstein, D., 1953, "An Investigation of Pressure-Drop Coefficients for Orifice Plates and Honeycomb Grids," MSc thesis, Georgia Institute of Technology, Atlanta, GA.
[26] Scheiman, J., 1981, "Considerations for the Installation of Honeycomb and Screens to Reduce Wind-Tunnel Turbulence," NASA Langley Research Center, Hampton, VA, Report No. NASA-TM-81868.
[27] Aufderheide, T., Bode, C., Friedrichs, J., and Kozulovic, D., 2014, "The Generation of Higher Levels of Turbulence in a Low-Speed Cascade Wind Tunnel by Pressurized Tubes," VI European Conference on Computational Fluid Dynamics (ECFD), Barcelona, Spain, July 20–25.
[28] Han, J.-C., Dutta, S., and Ekkad, S., 2012, *Gas Turbine Heat Transfer and Cooling Technology*, CRC Press, Boca Raton, FL.
[29] Hylton, L., Mihelc, M. S., Turner, E. R., Nealy, D. A., and York, R. E., 1983, "Analytical and Experimental Evaluation of the Heat Transfer Distribution Over the Surfaces of Turbine Vanes," Detroit Diesel Allison, Indianapolis, IN, Report No. NASA-CR-168015.
[30] Hilditch, M. A., Smith, G. C., and Singh, U. K., 1998, "Unsteady Flow in a Single Stage Turbine," ASME Paper No. 98-GT-531.
[31] Goethert, B. H., 1961, "Transonic Wind Tunnel Testing," DTIC Document, Dover Publications, Mineola, NY.
[32] Paniagua, G., Cuadrado, D., Saavedra, J., Andreoli, V., Meyer, T., Meyer, S., and Lawrence, D., 2016, "Design of the Purdue Experimental Turbine Aerothermal Laboratory for Optical and Surface Aero-Thermal Measurements," ASME Paper No. GT2016-58101.
[33] Chue, S., 1975, "Pressure Probes for Fluid Measurement," Prog. Aerosp. Sci., **16**(2), pp. 147–223.
[34] Shiau, C.-C., Chen, A. F., Han, J. C., Azad, S., and Lee, C. P., 2015, "Full-Scale Turbine Vane End-Wall Film-Cooling Effectiveness Distribution Using PSP Technique," ASME Paper No. GT2015-42206.
[35] Bogard, D., and Thole, K., 2006, "Gas Turbine Film Cooling," J. Propul. Power, **22**(2), pp. 249–270.
[36] Flegel, A. B., Welch, G. E., Giel, P. W., Ames, F. E., and Long, J. A., 2015, "Complementary Aerodynamic Performance Datasets for Variable Speed Power Turbine Blade Section From Two Independent Transonic Turbine Cascades," International Symposium on Air Breathing Engines (ISABE), Phoenix, AZ, Oct. 25–30, Paper No. ISABE 2015-20163.